ALK Mutants in the Kinase Domain Exhibit Altered Kinase Activity and Differential Sensitivity to Small Molecule ALK Inhibitors[†,¨]

Lihui Lu, Arup K. Ghose, Matthew R. Quail, Mark S. Albom, John T. Durkin, Beverly P. Holskin, Thelma S. Angeles, Sheryl L. Meyer, Bruce A. Ruggeri, and Mangeng Cheng*

Worldwide Discovery Research, Cephalon Inc., West Chester, Pennsylvania 19380

Received November 12, 2008; Revised Manuscript Received February 26, 2009

ABSTRACT: Abnormal expression of constitutively active anaplastic lymphoma kinase (ALK) chimeric proteins in the pathogenesis of anaplastic large-cell lymphoma (ALCL) is well established. Recent studies with small molecule kinase inhibitors have provided solid proof-of-concept validation that inhibition of ALK is sufficient to attenuate the growth and proliferation of *ALK* (+) ALCL cells. In this study, several missense mutants of ALK in the phosphate anchor and gatekeeper regions were generated and their kinase activity was measured. NPM-ALK L182M, L182V, and L256M mutants displayed kinase activity in cells comparable to or higher than that of NPM-ALK wild type (WT) and rendered BaF3 cells into IL-3-independent growth, while NPM-ALK L182R, L256R, L256V, L256P, and L256Q displayed much weaker or little kinase activity in cells. Similar kinase activities were obtained with corresponding GST-ALK mutants with in vitro kinase assays. With regard to inhibitor response, NPM-ALK L182M and L182V exhibited sensitivity to a fused pyrrolocarbazole (FP)-derived ALK inhibitor comparable to that of NPM-ALK WT but were dramatically less sensitive to a diaminopyrimidine (DAP)-derived ALK inhibitor. On the other hand, NPM-ALK L256M exhibited >30-fold lower sensitivity to both FP-derived and DAP-derived ALK inhibitors. The growth inhibition and cytotoxicity of BaF3/NPM-ALK mutant cells induced by ALK inhibitors were consistent with inhibition of cellular NPM-ALK autophosphorylation. In a mouse survival model, treatment with the orally bioavailable DAP-ALK inhibitor substantially extended the survival of the mice inoculated with BaF3/NPM-ALK WT cells but not those inoculated with BaF3/NPM-ALK L256M cells. Binding of ALK inhibitors to ALK WT and mutants was analyzed using ALK homology models. In summary, several potential active ALK mutants were identified, and our data indicate that some of these mutants are resistant to select small molecule ALK inhibitors. Further characterization of these mutants may help to identify and develop potent ALK inhibitors active against both WT and resistant mutants of ALK.

Targeted protein tyrosine kinase (PTK)[1] inhibitors represent a major advance in cancer treatment, and eight PTK inhibitors have been approved for the treatment of various cancer types (*1*−*7*). Although kinase inhibitors have been extremely effective in specific patient populations with tumors containing mutated, oncogenic forms of PTK, clinical studies thus far have indicated that most patients eventually develop resistance to these drugs. Resistance can be caused by various mechanisms, such as amplification of the targeted oncogenic PTK gene or other oncogenic protein kinases. In a majority of cases, however, resistance results from the selection of cancer cells with mutations in the targeted PTK, often in the kinase catalytic domain, leading to impairment of its interaction with the inhibitor (*8*−*10*). Resistant mutations have been observed in the kinase domain of BCR-ABL, Kit, and the platelet-derived growth factor receptor (PDGFR) in patients treated with imatinib, and in the epidermal growth factor receptor (EGFR) in patients treated with gefitinib or erlotinib (*8*−*14*).

Anaplastic lymphoma kinase (ALK) is a receptor tyrosine kinase that was first identified as part of the NPM-ALK fusion protein derived from a chromosomal translocation detected in the majority of anaplastic large cell lymphoma (ALCL) patients (*15*−*17*). Recently, it has been implicated as an oncogene in a subset of non-small cell lung cancers (NSCLC) harboring *EML4*−*ALK* fusion genes (*18, 19*) and in neuroblastoma due to mutation and amplification of the full-length ALK receptor (*20*−*24*). Although the precise physiological function and regulation of ALK have not been well defined, *ALK* fusion genes, such as *NPM-ALK* in ALCL or *EML4*−*ALK* in NSCLC, encode chimeric oncoproteins with constitutively active ALK tyrosine kinase activity, which play a key role in tumorigenesis by the aberrant phospho-

[†,¨] Supported by Cephalon Inc.

* To whom correspondence should be addressed. E-mail: mcheng@cephalon.com. Phone: (610) 738-6482. Fax: (610) 738-6755.

[1] Abbreviations: ALK, anaplastic lymphoma kinase; ALCL, anaplastic large-cell lymphoma; NPM, nucleophosmin; GST, glutathione *S*-transferase; TBS, Tris-buffered saline; PTK, protein tyrosine kinase; PDGFR, platelet-derived growth factor receptor; EGFR, epidermal growth factor receptor; BCR-ABL, breakpoint-cluster region-Abelson leukemia-virus protein; NSCLC, non-small cell lung cancer; FBS, fetal bovine serum; DSMZ, Deutsche Sammlung von Mikroorganismen and Zellkulturen GmbH; ATCC, American type Culture Collection; PCR, polymerase chain reaction; IGF-1R, insulin-like growth factor-1 receptor; LCK, leukocyte cell-specific kinase; FP, fused pyrrolocarbazole; DAP, diaminopyrimidine; EML4, echinoderm microtubule-associated protein-like 4.

10.1021/bi8020923 CCC: $40.75
Published on Web 02/27/2009

Phosphate anchor region

NPM-ALK	I^{176}	T	L	I	R	G	**L**	G	H	G	A	F	G
ABL1	I^{242}	T	M	K	H	K	**L**	G	G	G	Q	Y	G
PDGFRB	L^{600}	V	L	G	R	T	**L**	G	S	G	A	F	G
KIT	L^{589}	S	F	G	K	T	**L**	G	A	G	A	F	G
EGFR	F^{712}	K	K	I	K	V	**L**	G	S	G	A	F	G

Gatekeeper region

NPM-ALK	L^{250}	P	R	F	I	L	**L**	E	L	M	A	G	G
ABL1	P^{309}	P	F	Y	I	I	**T**	E	F	M	T	Y	G
PDGFRB	G^{675}	P	I	Y	I	I	**T**	E	Y	C	R	Y	G
KIT	G^{664}	P	T	L	V	I	**T**	E	Y	C	C	Y	G
EGFR	S^{784}	T	V	Q	L	I	**T**	Q	L	M	P	F	G

FIGURE 1: Alignment of sequences around the phosphate anchor and gatekeeper regions of NPM-ALK and select protein tyrosine kinases. The amino acid sequences around the phosphate anchor region and gatekeeper region of NPM-ALK, ABL1, PDGFRB, Kit, and EGFR were aligned and compared.

rylation of multiple intracellular downstream substrates (*15*−*17*). Several small molecule ALK inhibitors have been reported recently, and studies with these inhibitors have provided solid proof-of-concept validation that inhibition of ALK is sufficient to attenuate the growth and proliferation of *ALK* (+) ALCL cells and *EML4-ALK* (+) NSCLC cells (*16, 19, 25*−*28*).

Although a robust clinical response of ALCL patients to an ALK inhibitor is expected, some of those patients are also anticipated to develop resistance to the ALK inhibitor, most likely associated with single-point mutations in the kinase domain of ALK. Identification of the active mutants that are resistant to the first line ALK inhibitors will be useful in the rational design of more effective inhibitors.

In this study, several mutants of a leucine in the phosphate anchor region or of the gatekeeper leucine of ALK were generated and evaluated for their kinase activity in vitro as well as in cells and their responses to small molecule ALK inhibitors. These positions were chosen because they are in the conserved regions where most of the active mutants reported in BCR-ABL and EGFR have been found. ALK homology models were generated to illustrate the modes of binding of the ALK inhibitors to ALK WT and mutants.

MATERIALS AND METHODS

Cell Lines, Compounds, and Antibodies. The Sup-M2 cells (catalog no. ACC 509) and BaF3 cells (catalog no. ACC 300), both purchased from DSMZ (Heidelberg, Germany), were cultured in RPMI with 10% fetal bovine serum (FBS) and in RPMI with 10% FBS and 5−10 ng/mL murine interleukin-3 (IL-3; catalog no. 403-ML, R&D Systems, Minneapolis, MN), respectively. Chinese hamster ovary (CHO) cells were purchased from ATCC (CHO-K1; catalog no. CCL-61) and cultured in DMEM with 10% FBS.

The small molecule ALK inhibitor compound 1 (cmpd 1), 2-methyl-11-(2-methylpropyl)-4-oxo-4,5,6,11,12,13-hexahydro-2*H*-indazolo[5,4-*a*]pyrrolo[3,4-*c*]carbazol-8-yl [4-(dimethylamino)benzyl]carbamate, was described previously (*25*). Compound 13 (cmpd 13), (1*S*,2*S*,3*R*,4*R*)-3-({5-chloro-2-[(1-ethyl-2,3,4,5-tetrahydro-6-methoxy-2-oxo-1*H*-1-benzazepin-7-yl)amino]-4-pyrimidinyl}amino)bicyclo[2.2.1]hept-5-ene-2-carboxamide, was synthesized according to the procedures detailed previously (*29*).

Table 1: Relative Kinase Activities of NPM-ALK Mutants in Cells[a]

NPM-ALK	relative kinase activity in CHO cells with transient transfection	relative kinase activity in stable BaF3 cell lines
WT	100	100
L182M	30 ± 9	58 ± 10
L182V	35 ± 12	61 ± 16
L182R	20 ± 9	NA[b]
L256M	175 ± 23	317 ± 58
L256V	10 ± 8	NA[b]
L256R	<5	NA[b]
L256P	<5	NA[b]
L256Q	<5	NA[b]

[a] CHO cells were transfected with pCMV-Tag2B-NPM-ALK WT or mutants, and 48 h later, the cells were collected and phospho- and total NPM-ALK were detected by immunoblot analysis. The bands were quantitated, and the level of relative NPM-ALK phosphorylation (phospho-NPM-ALK/NPM-ALK ratio) was calculated. BaF3 cells were transfected with pCMV-Tag2B-NPM-ALK WT and mutants, and 48 h post-transfection, the cells were selected in culture medium with 800 μM G418 for 2−3 weeks without IL-3. The relative NPM-ALK phosphorylation was detected and calculated as described for CHO cells. The activity of each mutant relative to WT was reported as the average ± standard deviation from two or three individual experiments. [b] Not available since stable cell lines could not be generated.

The rabbit phospho-NPM-ALK (Y664) (catalog no. 3341) and ALK antibodies (catalog no. 3342) were purchased from Cell Signaling Technology (Beverly, MA). The actin antibody (catalog no. SC-1616) was supplied by Santa Cruz Biotechnology (Santa Cruz, CA).

The DNA oligos were synthesized and purified by Operon Biotechnologies Inc. (Huntsville, AL).

Mutagenesis and Cell Transfection. The NPM-ALK mutants were generated with the QuikChange site-directed mutagenesis kit (catalog no. 200523, Stratagene, La Jolla, CA) according to the manufacturer's instructions, with pCMV-Tag2B-NPM-ALK WT as the template. Each individual mutation was confirmed by DNA sequencing.

CHO cells were transfected with Lipofectamine 2000 transfection reagent (catalog no. 11668027, Invitrogen, Carlsbad, CA) according to the manufacturer's protocol.

BaF3/NPM-ALK mutant cell lines were generated by transfecting BaF3 cells with pCMV-Tag2B-NPM-ALK mutant DNA by the NucleoFector device, and the transfectants were then selected with G418 for 2−3 weeks in RPMI and 10% FBS without IL-3.

Recombinant GST−ALK Protein Production. Mutations corresponding to some of those in NPM-ALK were also introduced into a GST−ALK(1073−1458) fusion protein produced in insect cells. The mutations were created in the pFastBac-GST-ALK (1073−1458) transfer vector, generated from pFastBac-GST-ALK(1058−1620) (*25*), using the QuikChange multisite directed mutagenesis kit (Stratagene), with a second silent mutation added to give each construct a unique restriction map. Mutations and the entire cDNA sequence were confirmed by DNA sequencing. Recombinant baculoviruses were generated from the pFastBac vector using the Bac-to-Bac kit (Invitrogen) as directed. The GST−ALK(1073−1458) fusion proteins were expressed in Sf21 insect cells (obtained from the Boyce Thompson Institute, Ithaca, NY) grown in shake flasks containing EX-CELL 420 medium (Sigma-Aldrich, St. Louis, MO) at 27 °C and purified by glutathione affinity chromatography (*25*).

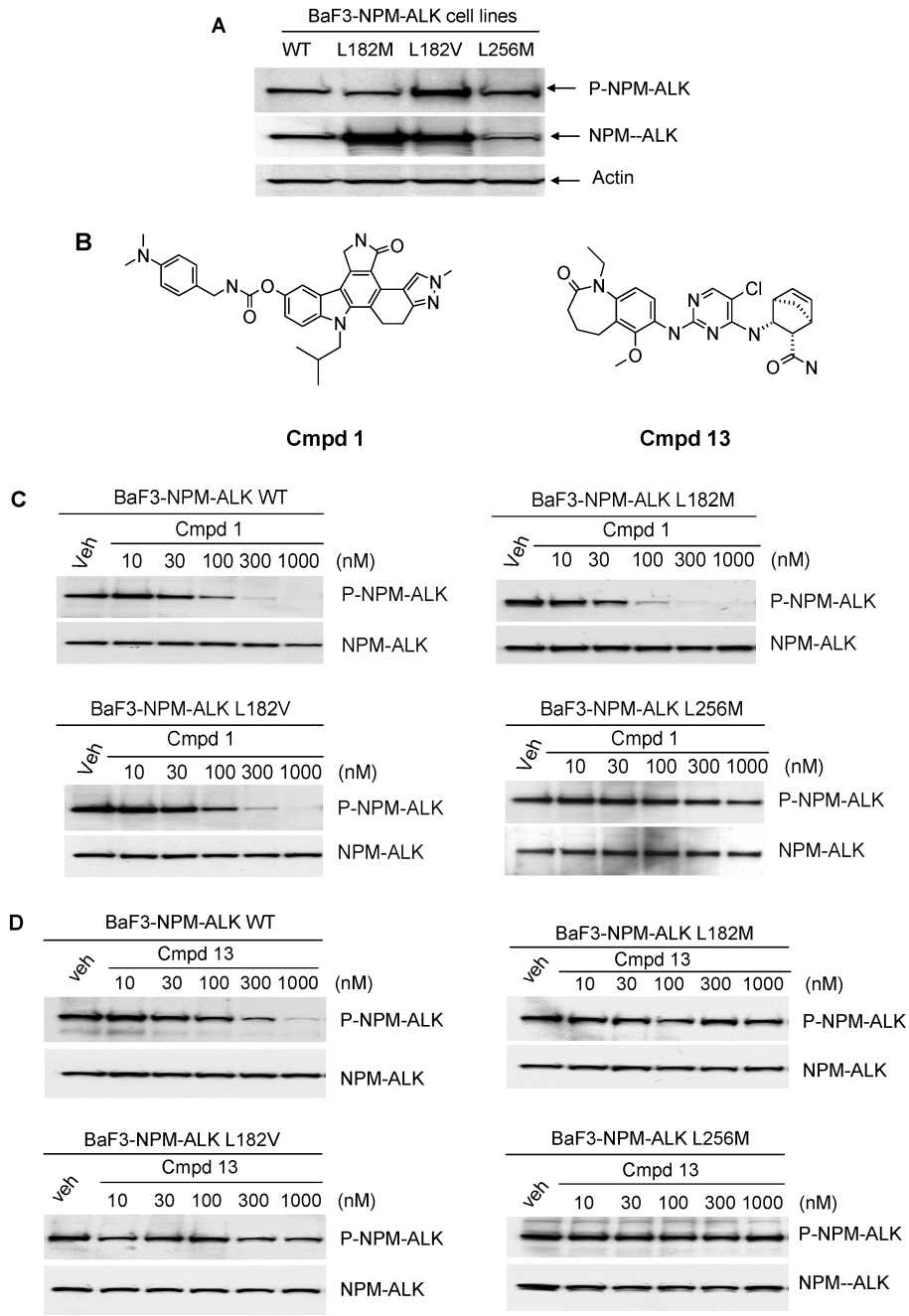

FIGURE 2: Tyrosine phosphorylation inhibition of NPM-ALK WT and mutants by ALK inhibitors in BaF3 cells. (A) Phospho-NPM-ALK and NPM-ALK levels of WT and mutants in BaF3 cells. The BaF3/NPM-ALK WT and mutant cells were lysed, and the lysates were resolved by SDS−PAGE. After being transferred, proteins were detected with either phospho-ALK or ALK antibody as described in Materials and Methods. (B) Structures of cmpd 1 and cmpd 13. (C and D) Tyrosine phosphorylation inhibition of NPM-ALK WT and mutants by ALK inhibitors. The BaF3/NPM-ALK WT and the mutant cells seeded in 12-well plates were treated with comp 1 or comp 13 at indicated concentrations for 2 h; the cells were then lysed, and the lysates were resolved via SDS−PAGE. After being transferred, proteins were detected with either phospho-ALK or total ALK antibody as described in Materials and Methods.

Recombinant GST−ALK Kinase Assay. The in vitro kinase assay for recombinant GST−ALK utilized a protein substrate, recombinant GST/human PLC-γ(541−852), in a time-resolved fluorescence (TRF)-based detection system as previously described (*25*). Comparison of the kinase activity of GST−ALK WT and mutants was carried out at 37 °C for 15 min in 100 μL of a reaction mixture consisting of 20 mM HEPES (pH 7.2), saturating ATP (200 μM), 5 mM $MnCl_2$, 0.1% BSA, and enzyme (GST−ALK WT or mutant). The phosphorylated product was then detected with Eu-N1-labeled PT66 antibody (catalog no. AD0041, PerkinElmer Life Sciences, Boston, MA). Following 1 h incubation at 37 °C, enhancement solution (catalog no. 1244-105, PerkinElmer Life Sciences, Boston, MA) was added. The plate was gently agitated, and after 10 min, the fluorescence of the resulting solution was measured using the PerkinElmer EnVision 2100 (or 2102) multilabel plate reader.

Immunoblot Analysis and MTS Assays. Immunoblot analysis of phospho-NPM-ALK and NPM-ALK was carried out according to the protocols provided by the antibody suppliers. In brief, the cells were lysed in Frak lysis buffer [10 mM Tris (pH 7.5), 1% Triton X-100, 50 mM sodium chloride, 20 mM sodium fluoride, 2 mM sodium pyrophosphate, 0.1% BSA, freshly prepared 1 mM activated sodium vanadate, 1

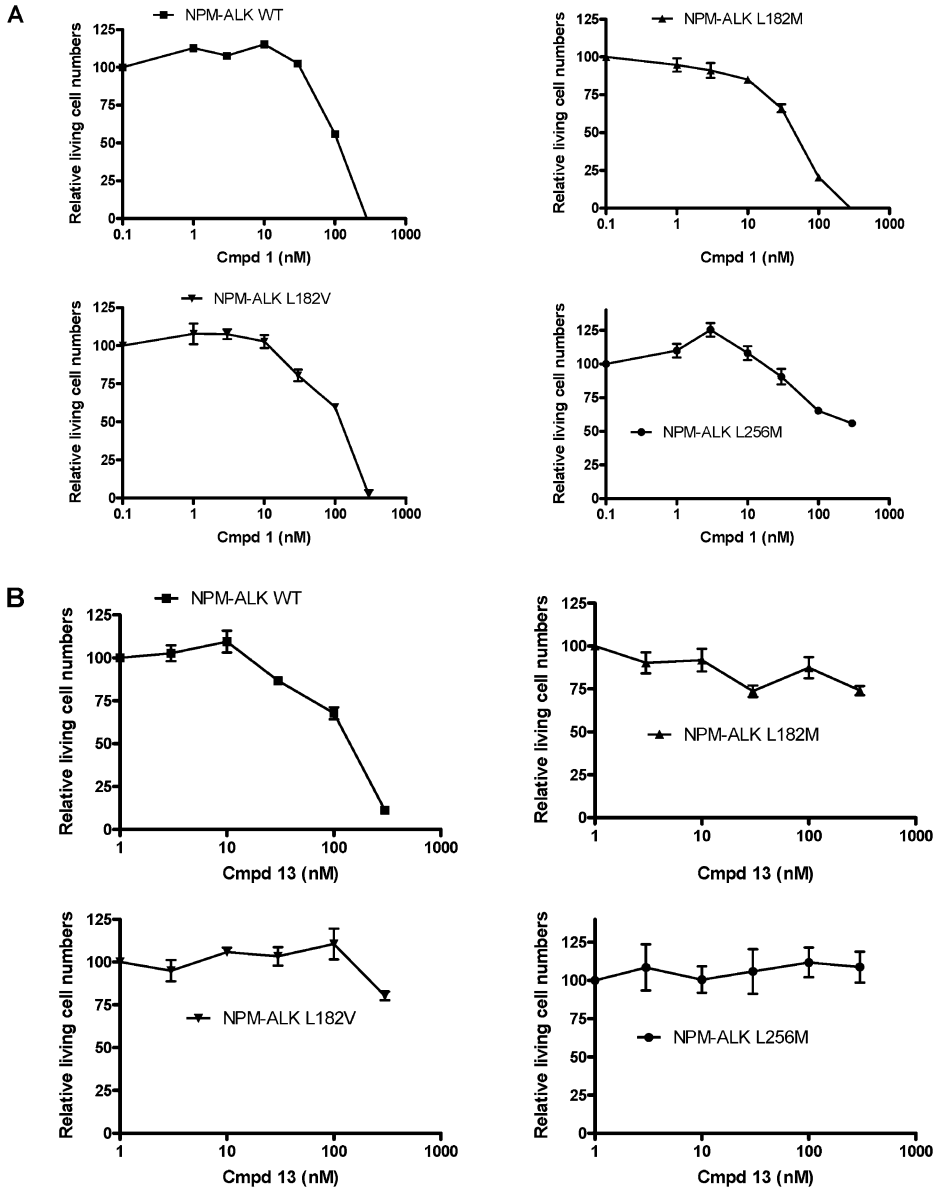

FIGURE 3: Growth inhibition of BaF3/NPM-ALK WT and mutant cells by cmpd 1 and cmpd 13. The BaF3/NPM-ALK WT and mutant cell lines were seeded on 96-well plates and treated with cmpd 1 (A) or cmpd 13 (B) at the indicated concentrations for 48 h. An equal volume of reagents from the CellTiter 96 Aqueous MTS kit was added to the culture medium, and the absorbance at 490 nm was measured with a plate reader. The number of living cells was calculated on the basis of the standard curve of each cell line. The values presented are the average of relative living cell numbers from two to three independent experiments with the standard error.

mM DTT, 1 mM PMSF, and protease inhibitor cocktail set III (1:100 dilution; catalog no. 539134 L; EMD Chemicals, Gibbstown, NJ)]. Following a brief sonication, the lysates were cleared by centrifugation, and the resulting supernatants were transferred to fresh tubes containing 4× LDS sample buffer (catalog no. NP0007, Invitrogen). The samples were heat-inactivated, and each sample was resolved by NuPAGE 7% Tris-acetate gels (catalog no. EA03552Box, Invitrogen). The gels were transferred to nitrocellulose membranes (catalog no. LC2000, Invitrogen), and after being blocked in Tris-buffered saline containing 0.2% Tween 20 (TBST) and 3% nonfat milk for 1 h, the membranes were incubated with anti-phospho-ALK antibody and, subsequently, the corresponding HRP-conjugated secondary antibody. After being washed, the membranes were incubated with ECL-Western blotting detection reagents (catalog no. RPN2106, GE Healthcare UK, Buckinghamshire, U.K.) and exposed to Kodak chemiluminescence BioMax films (catalog no. 178,8207, Carestream Health Inc., Rochester, NY), which were developed. The membranes were then stripped by incubation with stripping buffer [62.5 mM Tris HCl (pH 6.8), 2% SDS, and 100 mM 2-mercaptoethanol] for 30 min at 56 °C and reblotted with an anti-ALK antibody as described above for the phospho-ALK antibody. The films were scanned with a scanner, and the individual band of phospho- and total NPM-ALK was quantitated with Gel-Pro Analyzer (Media Cybernetics, Inc., Bethesda, MD).

Living cells were measured with the CellTiter 96 AQ_{ueous} nonradioactive cell proliferation assay kit (MTS kit) (catalog no. G5430, Promega, Madison, WI). In brief, the cells were seeded on 96-well plates, and 48 h after compound treatment, an equal volume of reagents from the kit was added to the culture medium. Absorbance at 490 nm was measured with a plate reader, and the relative number of living cells was calculated on the basis of the standard curve for the individual cell line.

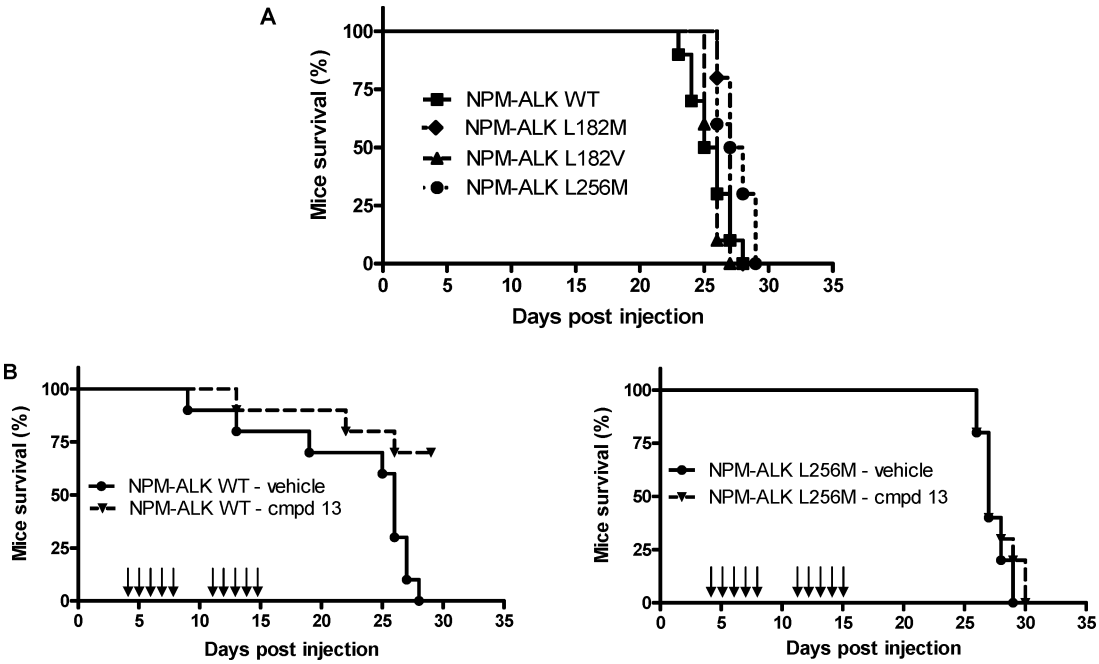

FIGURE 4: Survival rate of mice inoculated intraperitoneally with BaF3/NPM-ALK WT and mutant cells and the survival rate of tumor-bearing mice treated with cmpd 13. (A) Scid-Beige mice were inoculated intraperitoneally with 2×10^6 BaF3/NPM-ALK WT or mutant cells. The mice were then observed daily, and the survival rate was recorded. (B) Four days after being inoculated intraperitoneally with BaF3/NPM-ALK WT or L256M cells, the mice were inoculated orally with cmpd 13 at 55 mg/kg, bid for 10 days (↓). The mice were then monitored daily until all the mice in vehicle-treated group died, and the survival rate was recorded for each group.

RNA Preparation, PCR, and Sequencing. For RNA preparation, 5×10^6 cells were collected and the total RNA was obtained by using the RNeasy Mini Kit (catalog no. 74104, Qiagen, Valencia, CA) and quantitated by measuring its absorbance at 260 nm. Single-stranded cDNA was synthesized from total RNA using a QuantiTect reverse transcription kit (catalog no. 205311, Qiagen) according to the manufacturer's protocol. Polymerase chain reaction (PCR) amplifications were carried out by using the GeneAmp High Fidelity PCR System (catalog no. 4328216, Applied Biosystems, Foster City, CA) with 2 ng of cDNA and a 5′ primer (GGTTCAGGGCCAGTGCATATTAGTG) and a 3′ primer (CCTCCAAATACTGACAGCCACAGGC). The PCR products were purified with the QIAquick PCR purification kit (catalog no. 28104, Qiagen), and the sequences were determined by NAPCORE at the Children's Hospital of Philadelphia. The sequencing results were visualized with the sequence scanner software from Applied Biosystems.

Survival Study in Mice. Scid-Beige mice (Taconic, Hudson, NY) were inoculated intraperitoneally with 2×10^6 BaF3/NPM-ALK WT or mutant cells. The mice were then observed daily, and the survival rate was recorded. For compound treatment, the mice were inoculated intraperitoneally with BaF3/NPM-ALK WT or L256M cells, and 4 days after inoculation, the mice were dosed orally with cmpd 13 at 55 mg/kg, bid for 10 days. The mice were then monitored daily until all the mice in the vehicle-treated group died, and the survival rate was recorded for each group.

ALK Homology Modeling. Several ALK homology models were built using Schrodinger-Prime (Prime: Structure Prediction, Schrodinger Inc., New York, NY) and Tripos-Orchestrar (Orchestrar, Tripos, St. Louis, MO). The knowledge-based approach (*30*) suggested that cmpd 1 had a better chance of binding to a DFG-out form of the kinase while cmpd 13 would bind to a DFG-in form. The DFG-in structure was built primarily from the insulin-like growth factor-1 receptor (IGF-1R) [Protein Data Bank (PDB) entry 2oj9], and the DFG-out structure was built primarily from leukocyte cell-specific kinase (LCK) (PDB entry 2ofv). The missing loops were built from other protein homologues as identified in Orchestrar. The Orchestrar run was initiated from the results of Tripos-Fugue software on the ALK kinase domain sequence.

ALK Inhibitor Docking. Initially, Schrodinger-Induced_Fit workflows (https://www.schrodinger.com/SolutionDescription.php?mID=15&sID=18&cID=0) were used to generate 20 top scoring binding poses. Induced_Fit-generated binding poses were screened using the PDB knowledge base to focus further studies of the binding. For structures like cmpd 1, where Induced_Fit could not come up with any reasonable binding pose, the PDB knowledge base was used to generate the initial binding pose. The initial binding poses were subjected to MacroModel/Embrace minimization to generate the protein−inhibitor complex structure to be used for the mutation studies.

Protein Mutation and Analysis of the Protein−Inhibitor Complex. The mutation of the amino acid residues and scanning of the side chain conformations with the rotamer library were conducted using various protein modeling tools available in the Tripos-Biopolymer (http://www.tripos.com/index.php?family=modules,SimplePage,sybyl_biopolymer) module. Each WT protein−inhibitor complex was subjected to MacroModel/Embrace minimization before the mutation study.

RESULTS

ALK Mutants Display Different Kinase Activity in Enzymatic and Cellular Assays. Several NPM-ALK mutations at Leu182 (L182M, L182V, and L182R) in the phosphate

Table 2: Relative Kinase Activities of Recombinant GST-ALK Mutants in Vitro[a]

GST-ALK (enzyme)	relative kinase activity of GST-ALK mutants
WT	100
L182M	49 ± 14
L182V	33 ± 7
L182R	17 ± 3
L256M	236 ± 15
L256V	59 ± 17
L256R	0.3 ± 0.1

[a] A comparison of the kinase activity of GST-ALK WT and mutants was performed as described in Materials and Methods. The activity of each mutant relative to WT was reported as the average ± standard deviation of at least three determinations.

anchor region and at Leu256 (L256M, L256V, L256R, L256P, and L256Q) in the gatekeeper region of NPM-ALK were introduced since these are the two regions conserved among most protein tyrosine kinases and mutations at these two positions are likely to retain kinase activity. For example, Leu182 of NPM-ALK corresponds to Leu230 in ABL and Leu718 in EGFR, and Leu256 of NPM-ALK corresponds to Thr315 in ABL and Thr790 in EGFR (Figure 1). Various active mutants have been reported in those two regions of BCR-ABL in chronic myelogeneous leukemia patients who became resistant to imatinib (*8, 10*). To reflect likely drug-resistant mutants, all the NPM-ALK mutants were generated by a single nucleotide change. As shown in Table 1, when transiently transfected into CHO cells, these NPM-ALK mutants exhibited different kinase activity based on relative autophosphorylation levels on the docking site Y664 residue of NPM-ALK. While NPM-ALK L256M exhibited increased activity over that of the wild type, NPM-ALK L182M, L182V, L182R, and L256V exhibited weaker but measurable ALK phosphorylation in cells. On the other hand, NPM-ALK L256R, L256P, and L256Q presented almost nondetectable kinase activity in CHO cells (see Figure S1 of the Supporting Information). When expressed in BaF3 cells, only NPM-ALK L182M, L182V, and L256M could render BaF3 cells independent of IL-3 for their proliferation and generate stable cell lines, consistent with the transient transfection results in CHO cells. In BaF3 cells, NPM-ALK L256M exhibited a more than 2-fold increase in kinase activity relative to WT, while NPM-ALK L182M and NPM-ALK L182V displayed kinase activity slightly lower but comparable (a less than 2-fold difference) to that of WT (Figure 2A and Table 1). Interestingly, the total NPM-ALK levels of the WT and mutants detected in the BaF3 cells are inversely related to their relative kinase activity, with the total NPM-ALK level for L182M and L182V being ~2−3-fold greater than the WT level and that of L256M being ~$^1/_2$ to $^1/_3$ of the WT level. This fact resulted in comparable total phospho-NPM-ALK levels among these BaF3 cell lines (Figure 2A), suggesting the total levels of active NPM-ALK expressed in BaF3 cells may be self-limited.

Recombinant GST-ALK enzymes corresponding to the mutations in the NPM-ALK proteins described above were also generated. The same amino acid numbering from the NPM-ALK chimera is used for clarity. The kinase activity of each mutant was evaluated using a protein substrate, recombinant GST/human PLC-γ(541−852), in a TRF-based assay (*25*). As shown in Table 2, the Leu182 mutants in the phosphate anchor (GST-ALK L182M, GST-ALK L182V, and GST-ALK L182R) all displayed weaker activity than WT, consistent with the NPM-ALK data for the Leu182 mutants (Table 1). In the gatekeeper region, GST-ALK L256M exhibited a kinase activity 2.4-fold of that of WT while both GST-ALK L256V and GST-ALK L256R exhibited much weaker activity (Table 2). These results corroborated the data obtained with the NPM-ALK L256 mutants in cells (Table 1).

Differential Sensitivity of NPM-ALK WT and Mutants to ALK Inhibitors. Two potent ALK inhibitors from two different chemical series were used in this study (Figure 2B). cmpd 1 is a fused pyrrolocarbazole (FP) derivative with a cellular IC_{50} of 10−30 nM for NPM-ALK phosphorylation in ALCL cells (*25*), and cmpd 13 is a diaminopyrimidine derivative with a cellular IC_{50} of 45 nM for NPM-ALK phosphorylation in ALCL cells (*29, 31*). As shown in Figure 2C, while NPM-ALK L182M and L282V mutants were still sensitive to the inhibition of tyrosine phosphorylation by cmpd 1 in cells, with IC_{50} values comparable to that of WT (10−30 nM), the NPM-ALK L256M mutant conferred at least 30-fold lower sensitivity to the inhibition of tyrosine phosphorylation by cmpd 1 with an IC_{50} value of >1000 nM. On the other hand, all three NPM-ALK mutants, L182M, L182V, and L256M, were much less sensitive or resistant to the inhibition of tyrosine phosphorylation by cmpd 13 in cells, with IC_{50} values of >1000 nM (Figure 2D).

Consistent with ALK target inhibition in cells, treatment with cmpd 1 led to dose-dependent cytotoxicity and growth inhibition of BaF3 cells harboring NPM-ALK L182M and L182V in culture, similar to BaF3/NPM-ALK WT cells, and displayed much less cytotoxicity toward BaF3/NPM-ALK L256M cells in culture (Figure 3A). On the other hand, treatment with cmpd 13 at the concentrations that induced significant cytotoxicity and growth inhibition against BaF3/NPM-ALK WT cells did not have much effect on the growth and survival of BaF3/NPM-ALK L182M, L182V, and L256M cells (Figure 3B). These data indicate that certain NPM-ALK mutants may become less sensitive or resistant to an ALK inhibitor in a chemical scaffold-dependent fashion.

Differential Sensitivity of NPM-ALK WT and L256M Tumors to the DAP-ALK Inhibitor in Mice. It was reported that certain kinase domain mutants of BCR-ABL exhibited increased transformation potency, possibly due to altered substrate specificity and pathway activation in cells (*32*). To compare the tumor growth rate of BaF3/NPM-ALK WT and mutants in mice, equal numbers of BaF3/NPM-ALK WT or mutant cells were inoculated into Scid mice intraperitoneally. The mice inoculated with BaF3/NPM-ALK WT cells all developed tumors in the peritoneal cavity and died around the fourth week post injection. The mice inoculated with the BaF3/NPM-ALK mutant cells, L182M, L182V, or L256M, also developed tumors in the peritoneal cavity and died at approximately the same time as mice implanted with the WT cells (Figure 4A), indicating the tumors harboring NPM-ALK mutants had a comparable growth rate in Scid mice as the tumors bearing NPM-ALK WT.

Cmpd 13 is an orally bioavailable ALK inhibitor and is able to completely inhibit NPM-ALK tyrosine phosphorylation in subcutaneous ALCL tumor xenografts in Scid mice with an oral dose of 55 mg/kg (*31*). To compare the effect of treatment with cmpd 13 on the survival of mice inoculated

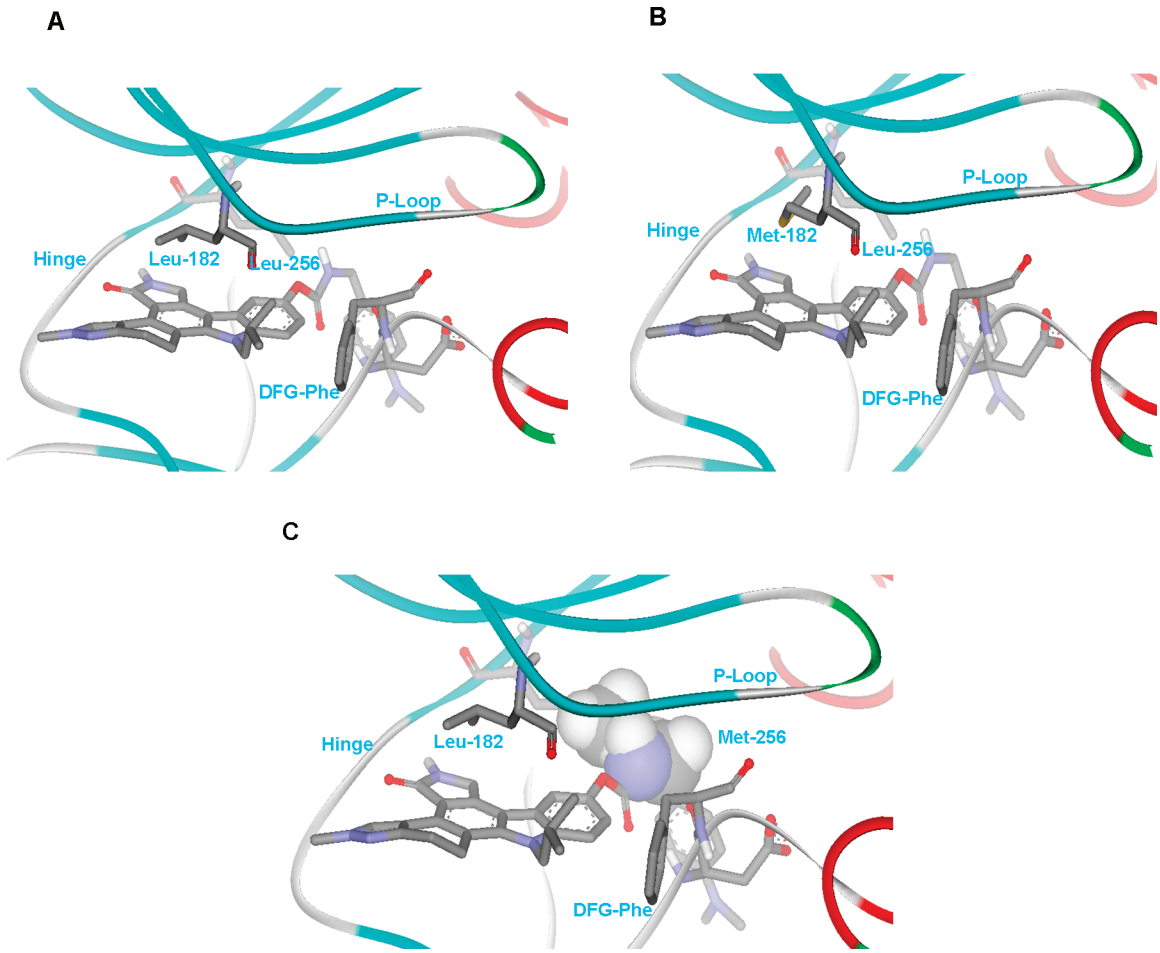

FIGURE 5: Basic mode of binding of cmpd 1 to DFG-out ALK WT (A) and mutants [(B) L182M and (C) L256M]. The ALK DFG-out model was derived from LCK (2ofv, 42.3% identical with ALK). The large carbamate substituent in cmpd 1 does not allow a binding mode with a DFG-in structure. It, however, fits nicely with a DFG-out structure with the known DFG-out hydrogen bonds and hydrophobic occupancy. (A) Mode of binding of cmpd 1 to ALK-WT without any steric clash. The locations of several critical residues for binding, including Leu182, Leu256, and the DFG motif, are shown. (B) Mode of binding of cmpd 1 to the ALK L182M mutant without any steric clash. (C) Mode of binding of cmpd 1 to the ALK L256M mutant, with one rotamer having direct clash with cmpd 1 shown here. The clashing region is shown with a CPK model.

with BaF3/NPM-ALK WT and L256M cells, 4 days after cell inoculation, the mice were treated with cmpd 13 at 55 mg/kg orally, bid for 10 days. Treatment of cmpd 13 significantly prolonged the survival of mice inoculated with BaF3/NPM-ALK WT cells, with 70% mice still alive when all the mice in the vehicle-treated group had died (Figure 4B). In contrast, treatment with cmpd 13 had no effect on the survival of mice inoculated with BaF3/NPM-ALK L256M cells and both vehicle- and cmpd 13-treated mice exhibited similar survival rates (Figure 4B). These data indicate that cmpd 13 effectively inhibits the growth and progression of tumors bearing NPM-ALK WT but not NPM-ALK L256M and substantiate the cellular data which show that NPM-ALK L256M is resistant to the inhibition by cmpd 13.

ALK Homology Modeling. ALK homology models were generated to illustrate the binding modes of the ALK inhibitors to ALK WT and mutants. It has been reported that compounds are able to bind to a protein kinase, such as p38a MAP kinase, in either the DGF-in or DGF-out conformation, depending on the substituents (*33*). Our earlier analysis of the DFG-out structures in the PDB suggested that two kinase residues might favor the formation of the DFG-out structure of the kinase, namely, (i) a small gatekeeper residue, usually a Thr, and (ii) Gly or Ala for X in XDFG (*30*). The gatekeeper in ALK is Leu, and X in ALK is Gly. c-MET is the only kinase with a Leu gatekeeper residue that has a DFG-out structure in the PDB. The X residue in c-MET is Ala. These observations supported the postulation of a DFG-out structure for ALK. Therefore, both ALK DFG-out and DFG-in homology models were generated. The ALK DFG-out model was derived from LCK (2ofv, 42.3% identical with ALK), while the ALK DFG-in model was derived from IGF-1R (2oj9, 47% identical with ALK). Even though the FP and DAP analogues are both known to bind to the DFG-in form of the kinases, the large *p*-NN-dimethylaminobenzyl-carbamate substituent in cmpd 1 did not allow any reasonable docking pose in the ALK DFG-in model. In contrast, the carbamate can form hydrogen bonds with the DFG-Asp backbone NH group in the DFG-out structure and the benzyl group can occupy the hydrophobic pocket previously occupied by the Phe of DFG in the DFG-in structure.

Inhibitor Docking and Mutation Analyses. The mode of binding of cmpd 1 to the ALK DFG-out model and the locations of a few important residues of ALK are shown in Figure 5A. There are a large number of FP-like inhibitors bound to different kinases in the PDB. Those inhibitors bind with the same binding mode to all kinases. In the current

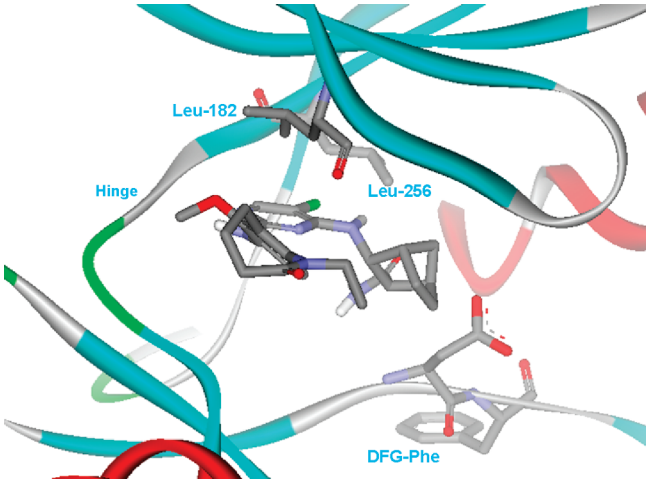

FIGURE 6: Mode of binding of cmpd 13 to the DFG-in ALK WT model. The ALK DFG-in model was derived from IGF-1R (2oj9, 47% identical with ALK). The binding mode was generated by the Schrodinger/Induced_Fit automated docking program, and the binding mode is consistent with the binding poses for DAP derivatives in the Protein Data Bank.

proposed binding mode, the X-ray crystallographically observed binding mode was preserved. However, the kinase was made DFG-out to accommodate the extra carbamate substituent. None of the FP-like inhibitors in the PDB had any substituent as in cmpd 1 that can trigger a DFG-out conformation for the kinases. To study the effect of individual ALK mutation on the binding mode, it was assumed that the basic binding mode of cmpd 1 and cmpd 13 would remain the same in these mutants. This is consistent with the recent analysis of the inhibitor-bound kinase structures in the PDB (*30*). Most kinase inhibitors, except for a few like imatinib, bind the same way with all kinases. The minor changes in the binding mode, such as the small movement of the inhibitor relative to different kinase residues, were studied by the constrained minimization of the kinase−inhibitor complexes. Ideally, one should expect that the computation of the interaction between the kinase (wild type or mutants) and an inhibitor will quantitatively predict the relative activities of the inhibitor. In reality, the current state of the discipline (*34*) is far from this ideal situation. Therefore, a qualitative approach, in which the mutated residue side chain conformation was scanned using Lovell's rotamer library (*35*), was used in this study. Identification of a rotamer without any steric clash or with a small steric clash might ensure that the protein would accommodate the ligand without any major change in structure. The torsional scanning of the library of rotamers showed that for cmpd 1, the L182M and L182V mutants had common side chain rotamers that did not have any steric congestion and were similar to the WT (Figure 5B and data not shown). In contrast, all side chain rotamers of the L256M mutant resulted in significant steric clash interfering with the binding of cmpd 1 (Figure 5C). This is consistent with the biochemical data in which cmpd 1 inhibited NPM-ALK L182M and L182V mutants, but not the NPM-ALK L256M mutant (Figure 2B). This result clearly suggested that the existence of a nonclashing low-energy rotamer of the mutant residue might be important for inhibitor binding.

From the initial Induced_Fit docking of cmpd 13 to the ALK DFG-in model, one docking pose, as shown in Figure 6, was chosen for further analysis. This binding mode is consistent with those proposed for other kinase-bound DAP analogues available in the PDB (1h01 and 1h08). Relative to cmpd 1, cmpd 13 is a more flexible compound and fits nicely in the DGF-in model but more loosely (Figure 6). For the L182M mutant, only a very small percentage (3%) of rotamers were found not to produce any steric clash, and such a small population is consistent with much lower target inhibition activity in the biochemical assay. Because of its more loose-fitting binding mode, the L182V mutant would tend to decrease the critical hydrogen bond strength as well as the hydrophobic interactions at the hinge region with cmpd 13, likely resulting in the less potent activity observed in the biochemical assay. The change to a fairly large residue, Met, in place of the gatekeeper Leu256 was also expected to result in rotamers with steric clash that adversely affected the binding of cmpd 13 (data not shown).

DISCUSSION

Point mutations in the kinase domain of PTKs, such as BCR-ABL, Kit, and EGFR, that impair drug binding have been established as the major mechanism of acquired resistance to these kinase inhibitor(s). Here we generated several ALK mutants in the kinase domain and evaluated their kinase activity and their sensitivity to the inhibition by different classes of ALK inhibitors. Of the gatekeeper mutants, only L256M had substantial kinase activity, approximately 3-fold of that of WT, both in cells and in the recombinant GST-ALK. This is consistent with the work of Azam et al. (*36*), in which introduction of the bulky methionine into the gatekeeper position of c-ABL, c-Src, PDGFRA/B, and EGFR resulted in the most active kinase. In addition to L256M, L182M and L182V displayed comparable kinase activity in cells relative to NPM-ALK WT, and all three NPM-ALK mutants were able to render BaF3 cells independent of IL-3 for their proliferation. NPM-ALK L182M and L182V exhibited sensitivity to an FP-derived ALK inhibitor comparable to that of NPM-ALK WT but were much less sensitive to a DAP-derived ALK inhibitor. On the other hand, NPM-ALK L256M displayed much less sensitivity or became resistant to both the FP-derived and DAP-derived ALK inhibitors. Consistent with inhibition of NPM-ALK autophosphorylation, the FP-ALK inhibitor induced growth inhibition and cytotoxicity of BaF3/NPM-ALK L182M and L182V cells but not L256M cells. In contrast, the DAP ALK inhibitor failed to induce growth inhibition and cytotoxicity of all three BaF3/NPM-ALK mutant cell lines in culture. In a mouse survival model, treatment with the orally bioavailable DAP-ALK inhibitor substantially prolonged the survival of the mice bearing BaF3/NPM-ALK WT tumors but not those with BaF3/NPM-ALK L256M tumors.

It has been reported that certain mutations create more potent BCR-ABL and may therefore accelerate disease progression (*31*). Although L256M was found to be hyperactive in the autophosphorylation of NPM-ALK kinase, BaF3 cells harboring this ALK mutant exhibited a growth rate similar to that of the BaF3/NPM-ALK WT cells in regular culture medium (Figure S3 of the Supporting Information). Also, a similar survival curve was observed in the systemic tumor models of BaF3 cells harboring NPM-ALK WT or

mutants in mice. Therefore, these data indicate that the NPM-ALK mutant cells may not present any growth advantage under those conditions.

NPM-ALK L182M and L182V mutants were found to remain sensitive to an ALK inhibitor derived from the FP chemical series but became resistant to an ALK inhibitor derived from a distinct DAP chemical series, suggesting that the binding modes of the two inhibitors to ALK may differ. The ALK homology modelings support that hypothesis, as cmpd 1 was predicted to bind to the DFG-out form while cmpd 13 was predicted to bind to a DFG-in form. These data also suggest that if the mutants in this region become resistant to the first line ALK inhibitor, it is likely that a compound(s) active against those mutants can be identified from a distinct chemical series. These results are consistent with the BCR-ABL mutants in the phosphate anchor region, which are found to be resistant to imatinib but sensitive to most of the second-generation ABL inhibitors, such as nilotinib and dasatinib. The ALK homology models suggest that an inhibitor with a large, flat, and rigid hinge binding moiety may be more likely to remain active against mutations in the hinge region than an inhibitor with a flexible hinge binding moiety. The fact that the NPM-ALK L256M mutant is resistant to the two ALK inhibitors derived from two distinct chemical classes suggests that it may be more challenging to identify a compound active against ALK mutants in the gatekeeper region. This observation reflects the case with the BCR-ABL T315I gatekeeper mutant, which is resistant to imatinib and almost all of the second-generation ABL inhibitors.

Although no resistant mutants of NPM-ALK and other ALK chimeras have been reported so far, with the influx of several small molecule ALK inhibitors into preclinical development and clinical trials for *ALK* (+) ALCL, NSCLC, and possibly neuroblastoma, it is expected that kinase inhibitor-resistant ALK mutants that would present excellent targets for developing second-generation ALK inhibitors will soon emerge. It will be interesting to determine whether any of the active ALK mutants described here emerge from primary tumor samples from patients treated clinically with ALK inhibitor(s).

The results generated with the NPM-ALK mutants here likely apply to other ALK chimeric proteins, such as EML4-ALK, since all the ALK chimeras contain the identical entire cytoplasmic domain of ALK. Recently, several ALK receptor missense mutations were found in neuroblastomas, and the mutations that were mapped to the critical region of the kinase domain were predicted to be oncogenic drivers (*21*−*24*). Since ALK is likely a tractable therapeutic target for neuroblastoma, it is imperative to test and compare the sensitivity of these ALK receptor mutants to the first generation of ALK inhibitors as well.

ACKNOWLEDGMENT

We thank Kristen Murray and Joann Caminiti for their excellent technical support and Mark Ator for critical review and comments about the manuscript.

SUPPORTING INFORMATION AVAILABLE

Expression and tyrosine phosphorylation levels of NPM-ALK WT and mutants in CHO cells, the caspase 3/7 activity in BaF3/NPM-ALK WT and L256M cells treated with cmpd 1 and cmpd 13, and the growth curve of BaF3/NPM-ALK WT and mutants cultured in medium containing 10% serum. This material is available free of charge via the Internet at http://pubs.acs.org.

REFERENCES

1. Druker, B. J. (2004) Imatinib as a paradigm of targeted therapies. *Adv. Cancer Res. 91*, 1–30.
2. Weisberg, E., Manley, P. W., Cowan-Jacob, S. W., Hochhaus, A., and Griffin, J. D. (2007) Second generation inhibitors of BCR-ABL for the treatment of imatinib-resistant chronic myeloid leukemia. *Nat. Rev. Cancer 7*, 345–356.
3. Quintas-Cardama, A., Kantarjian, H., and Cortes, J. (2007) Flying under the radar: The new wave of BCR-ABL inhibitors. *Nat. Rev. Drug Discovery 6*, 834–848.
4. Fong, T., Morgensztern, D., and Govindan, R. (2008) EGFR inhibitors as first-line therapy in advanced non-small cell lung cancer. *J. Thorac. Oncol. 3*, 303–310.
5. Motzer, R. J., Michaelson, M. D., Rosenberg, J., Bukowski, R. M., Curti, B. D., George, D. J., Hudes, G. R., Redman, B. G., Margolin, K. A., and Wilding, G. (2007) Sunitinib efficacy against advanced renal cell carcinoma. *J. Urol. 178*, 1883–1887.
6. Grandinetti, C. A., and Goldspiel, B. R. (2007) Sorafenib and sunitinib: Novel targeted therapies for renal cell cancer. *Pharmacotherapy 27*, 1125–1144.
7. Medina, P. J., and Goodin, S. (2008) Lapatinib: A dual inhibitor of human epidermal growth factor receptor tyrosine kinases. *Clin. Ther. 30*, 1426–1447.
8. Shah, N. P., and Sawyers, C. L. (2003) Mechanisms of resistance to STI571 in Philadelphia chromosome-associated leukemias. *Oncogene 22*, 7389–7395.
9. O'Hare, T., Eide, C. A., and Deininger, M. W. (2007) Bcr-Abl kinase domain mutations, drug resistance, and the road to the cure for chronic myeloid leukemia. *Blood 110*, 2242–2249.
10. Engelman, J. A., and Settleman, J. (2008) Acquired resistance to tyrosine kinase inhibitors during cancer therapy. *Curr. Opin. Genet. Dev. 18*, 1–7.
11. Liu, J., Joha, S., Idziorek, T., Corm, S., Hetuin, D., Philippe, N., Preudhomme, C., and Quesnel, B. (2008) BCR-ABL mutants spread resistance to non-mutated cells through a paracrine mechanism. *Leukemia 22*, 791–799.
12. Desai, J., Shankar, S., Heinrich, M. C., Fletcher, J. A., Fletcher, C. D., Manola, J., Morgan, J. A., Corless, C. L., George, S., Tuncali, K., Silverman, S. G., Van den Abbeele, A. D., van Sonnenberg, E., and Demetri, G. D. (2007) Clonal evolution of resistance to imatinib in patients with metastatic gastrointestinal stromal tumors. *Clin. Cancer Res. 13*, 5398–5405.
13. Corless, C. L., Schroeder, A., Griffith, D., Town, A., McGreevey, L., Harrell, P., Shiraga, S., Bainbridge, T., Morich, J., and Heinrich, M. C. (2008) PDGFRA mutations in gastrointestinal stromal tumors: Frequency, spectrum and in vitro sensitivity to imatinib. *J. Clin. Oncol. 23*, 5357–5364.
14. Engleman, J. A., and Janne, P. A. (2008) Mechanisms of acquired resistance to epidermal growth factor receptor tyrosine kinase inhibitors in non-small cell lung cancer. *Clin. Cancer Res. 14*, 2895–2899.
15. Pulford, K., Morris, S. W., and Turturro, F. (2004) Anaplastic lymphoma kinase proteins in growth control and cancer. *J. Cell. Physiol. 9*, 330–358.
16. Li, R., and Morris, S. W. (2008) Development of anaplastic lymphoma kinase (ALK) small-molecule inhibitors for cancer therapy. *Med. Res. Rev. 28*, 372–412.
17. Chiarle, R., Voena, C., Ambrogio, C., Piva, R., and Inghirami, G. (2008) The anaplastic lymphoma kinase in the pathogenesis of cancer. *Nat. Rev. Cancer 8*, 11–23.
18. Soda, M., Choi, Y. L., Enomoto, M., Takada, S., Yamashita, Y., Ishikawa, S., Fujiwara, S., Watanabe, H., Kurashina, K., Hatanaka, H., Bando, M., Ohno, S., Ishikawa., Y., Aburatani, H., Niki, T., Sohara, Y., Sugiyama, Y., and Mano, H. (2007) Identification of the transforming EML4-ALK fusion gene in non-small-cell lung cancer. *Nature 448*, 561–566.
19. Koivunen, J. P., Mermel, C., Zejnullahu, K., Murphy, C., Lifshits, E., Holmes, A. J., Choi, H. G., Kim, J., Chiang, D., Thomas, R., Lee, J., Richards, W. G., Sugarbaker, D. J., Ducko, C., Lindeman, N., Marcoux, J. P., Engelman, J. A., Gray, N. S., Lee, C., Meyerson,

M., and Jänne, P. A. (2008) EML4-ALK fusion gene and efficacy of an ALK kinase inhibitor in lung cancer. *Clin. Cancer Res. 14*, 4275–4283.
20. McDermott, U., Iafrate, A. J., Gray, N. S., Shioda, T., Classon, M., Maheswaran, S., Zhou, W., Choi, H. G., Smith, S. L., Dowell, L., Ulkus, L. E., Kuhlmann, G., Greninger, P., Christensen, J. G., Haber, D. A., and Settleman, J. (2008) Genomic alterations of anaplatic lymphoma kinase may sensitize tumors to anaplastic lymphoma kinase inhibitors. *Cancer Res. 68*, 3389–3395.
21. Mossé, Y. P., Laudenslager, M., Longo, L., Cole, K. A., Wood, A., Attiyeh, E. F., Laquaglia, M. J., Sennett, R., Lynch, J. E., Perri, P., Laureys, G., Speleman, F., Kim, C., Hou, C., Hakonarson, H., Torkamani, A., Schork, N. J., Brodeur, G. M., Tonini, G. P., Rappaport, E., Devoto, M., and Maris, J. M. (2008) Identification of ALK as a major familial neuroblastoma predisposition gene. *Nature 455*, 930–936.
22. Janoueix-Lerosey, I., Lequin, D., Brugières, L., Ribeiro, A., de Pontual, L., Combaret, V., Raynal, V., Puisieux, A., Schleiermacher, G., Pierron, G., Valteau-Couanet, D., Frebourg, T., Michon, J., Lyonnet, S., Amiel, J., and Delattre, O. (2008) Somatic and germline activating mutations of the ALK kinase receptor in neuroblastoma. *Nature 455*, 967–970.
23. Chen, Y., Takita, J., Choi, Y. L., Kato, M., Ohira, M., Sanada, M., Wang, L., Soda, M., Kikuchi, A., Igarashi, T., Nakagawara, A., Hayashi, Y., Mano, H., and Ogawa, S. (2008) Oncogenic mutations of ALK kinase in neuroblastoma. *Nature 455*, 971–974.
24. George, R. E., Sanda, T., Hanna, M., Fröhling, S., Luther, W., Zhang, J., Ahn, Y., Zhou, W., London, W. B., McGrady, P., Xue, L., Zozulya, S., Gregor, V. E., Webb, T. R., Gray, N. S., Gilliland, D. G., Diller, L., Greulich, H., Morris, S. W., Meyerson, M., and Look, A. T. (2008) Activating mutations in ALK provide a therapeutic target in neuroblastoma. *Nature 455*, 975–978.
25. Wan, W., Albom, M. S., Lu, L., Quail, M. R., Becknell, N. C., Weinberg, L. R., Reddy, D. R., Holskin, B. P., Angeles, T. S., Underiner, T. L., Meyer, S. L., Hudkins, R. L., Dorsey, B. D., Ator, M. A., Ruggeri, B. A., and Cheng, M. (2006) Anaplastic lymphoma kinase activity is essential for the proliferation and survival of anaplastic large-cell lymphoma cells. *Blood 107*, 1617–1623.
26. Christensen, J. G., Zou, H. Y., Arango, M. E., Li, Q., Lee, J. H., McDonnell, S. R., Yamazaki, S., Alton, G. R., Mroczkowski, B., and Los, G. (2007) Cytoreductive antitumor activity of PF-2341066, a novel inhibitor of anaplastic lymphoma kinase and c-Met, in experimental models of anaplastic large-cell lymphoma. *Mol. Cancer Ther. 6*, 3314–3322.
27. Galkin, A. V., Melnick, J. S., Kim, S., Hood, T. L., Li, N., Li, L., Xia, G., Steensma, R., Chopiuk, G., Jiang, J., Wan, Y., Ding, P., Liu, Y., Sun, F., Schultz, P. G., Gray, N. S., and Warmuth, M. (2007) Identification of NVP-TAE684, a potent, selective, and efficacious inhibitor of NPM-ALK. *Proc. Natl. Acad. Sci. U.S.A. 104*, 270–275.
28. Soda, M., Takada, S., Takeuchi, K., Choi, Y. L., Enomoto, M., Ueno, T., Haruta, H., Hamada, T., Yamashita, Y., Ishikawa, Y., Sugiyama, Y., and Mano, H. (2008) A mouse model for EML4-ALK-positive lung cancer. *Proc. Natl. Acad. Sci. U.S.A. 105*, 19893–19897.
29. Ahmed, G., Bohnstedt, A., Breslin, J. H. (2008) Fused bicyclic derivatives of 2,4-diaminopyrimidine as ALK and c-Met inhibitors. Patent WO/2008/051547.
30. Ghose, A. K., Herbertz, T., Pippin, D. A., Salvino, J. M., and Mallamo, J. P. (2008) Knowledge based prediction of ligand binding modes and rational inhibitor design for kinase drug discovery. *J. Med. Chem. 51*, 5149–5171.
31. Ott, G. R., Cheng, M., Tripathy, R., McHugh, R., Weinberg, L., Milkiewicz, K. L., Anzalone, A. V., Underiner, T. J., Curry, M. A., Breslin, H. J., Quail, M. R., Lu, L., Wan, W., Angeles, T. S., Albom, M. S., Aimone, L., Ator, M. A., Ruggeri, B. A., and Dorsey, B. D. (2008)Discovery of a potent, selective, orally bioavailable inhibitor of anaplastic lymphoma kinase with in vivo antitumor activity in animal models of anaplastic large-cell lymphoma (abstract). Translational Cancer Medicine 2008: Bridging the lab and the clinic in cancer medicine, Nov 3−6.
32. Griswold, I. J., Macpartlin, M., Bumm, T., Goss, V. L., O'Hare, T., Lee, K. A., Corbin, A. S., Stoffregen, E. P., Smith, C., Johnson, K., Moseson, E. M., Wood, L. J., Polakiewicz, R. D., Druker, B. J., and Deininger, M. W. (2006) Kinase domain mutants of Bcr-Abl exhibit altered transformation potency, kinase activity, and substrate utilization, irrespective of sensitivity to imatinib. *Mol. Cell. Biol. 26*, 6082–6093.
33. Angell, R. M., Angell, T. D., Bamborough, P., Bamford, M. J., Chung, C., Cockerill, S. G., Flack, S. S., Jones, K. L., Laine, D. I., Longstaff, T., Ludbrook, S., Pearson, R., Smith, K. J., Smee, P. A., Somers, D. O., and Walker, A. L. (2008) Biphenyl amide p38 kinase inhibitors 4: DFG-in and DFG-out binding modes. *Biomed. Chem. Lett. 18*, 4433–4437.
34. Leach, A. R., Shoichet, B. K., and Peishoff, C. E. (2006) Prediction of protein-ligand interactions. Docking and scoring: Successes and gaps. *J. Med. Chem. 49*, 5851–5855.
35. Lovell, S. C., Word, J. M., Richardson, J. S., and Richardson, D. C. (2000) The Penultimate Rotamer Library. *Proteins: Struct., Funct., Genet. 40*, 389–406.
36. Azam, M., Seeliger, M. A., Gray, M. S., Kuriyan, J., and Daley, G. Q. (2008) Activation of tyrosine kinases by mutation of the gatekeeper threonine. *Nat. Struct. Mol. Biol. 15*, 1109–1118.

BI8020923